Image–Guided *Ex vivo* Liver Ablation by Unfocused Ultrasound using Passive Cavitation Detection

Vasant A. Salgaonkar, Chandra Priya Karunakaran, John A. Besse, Grace Heinlein, Saurabh Datta, Christy K. Holland, T. Douglas Mast
Department of Biomedical Engineering, University of Cincinnati, Cincinnati, Ohio

ABSTRACT

Ablation therapy is used as an alternative to surgical resection of hepatic tumors. In ablation, tumors are destroyed through heating by RF current, high intensity focused ultrasound (HIFU), or other energy sources. Ablation can be performed with a linear array transducer delivering unfocused intense ultrasound (>10 W/cm^2). This allows simultaneous treatment and imaging, a feature uncommon in RF ablation. Unfocused ultrasound can also enable faster bulk tissue ablation than HIFU.

In the experiments reported here, a 32-element linear array transducer with a 49 mm aperture delivers 3.1 MHz continuous wave unfocused ultrasound at amplitudes 0.7–1.4 MPa during the therapy cycle. It also operates in pulse-echo mode to capture B-scan images. *Ex-vivo* fresh bovine liver tissue placed in degassed saline is exposed to continuous wave ultrasound interleaved with brief pulsed ultrasound imaging cycles. Tissue exposures range between 5 to 20 minutes. The following measurements are made at intervals of 1 to 3 seconds: tissue temperature with a needle thermocouple, acoustic emissions with a 1 MHz passive unfocused detector, and tissue echogenicity from image brightness.

Passively detected acoustic emissions are used to quantify cavitation activity in the ablation experiments presented here. As severity and extent of tissue ablation are related to temperature, this paper will statistically model temperature as a function of tissue echogenicity and cavitation. The latter two quantities can potentially be monitored noninvasively and used as a surrogate for temperature, enabling improved image guidance and control of ultrasound ablation.

KEYWORDS: Ultrasound ablation, Cavitation, Logistic regression, Temperature, Monitoring, Statistical Modeling

1. INTRODUCTION

Thermal ablation is widely used for treatment of nonresectable tumors of the liver and other soft tissue. Radiofrequency ablation (RFA) is most common, but other energy modalities including ultrasound are used too.[1,2] The use of intense ultrasound for tissue ablation described in this paper is derived from Makin *et al.* (2005), where a miniaturized ultrasound array performs interleaved tissue ablation and imaging. This is a minimally invasive treatment modality which can be used for bulk ablation of large tumors and can achieve performance comparable to RFA.[3] The ability to control energy delivery and estimate the corresponding bioeffects are key aspects of an effective ablation treatment. Ability to monitor tissue temperature noninvasively can assist in treatment control. Cavitation activity resulting from ultrasound exposures may play a role in heat deposition and lesion formation.[4] This, along with tissue echogenicity can be recorded noninvasively. An *ad hoc* mathematical model which can estimate tissue temperature, given the cavitation activity and tissue echogenicity may enable noninvasive temperature monitoring.

Passive cavitation detection in high–intensity focused ultrasound (HIFU) exposures and the role of cavitation in ablative lesion formation has been studied experimentally in recent years. It has been reported that subharmonic and broadband acoustic emissions were indicative of stable bubble oscillations and inertial bubble collapse respectively.[5] Low frequency acoustic emissions (in kHz range) have been used to detect tissue boiling during HIFU exposures by

Thermal Treatment of Tissue: Energy Delivery and Assessment IV, edited by Thomas P. Ryan,
Proc. of SPIE Vol. 6440, 64400Q, (2007) · 1605-7422/07/$18 · doi: 10.1117/12.701029

Anand *et al.*[6] Changes in tissue echogenicity as result of cavitation have been studied for HIFU exposures by Rabkin *et al.*[7] Physical dynamics of cavitation activity in relation to tissue temperature have been studied under HIFU conditions by Thomas *et al.*[8] Analytical methods which model the physical phenomenon of heat deposition during ultrasound ablation have been presented by Mast *et al.* for unfocused ultrasound ablation.[9]

The objective of the work reported here was to explore the correlation of cavitation and tissue echogenicity with ablative efficacy (or temperature), with the intent of exploiting cavitation activity for treatment monitoring and control by employing a statistical framework. Passive cavitation detection was performed during tissue ablation experiments using intense unfocused ultrasound in MHz range at the University of Cincinnati.[10] Acoustic emissions were recorded and tissue echogenicity was calculated from B-scan images. In this paper, statistical input/output models are derived based on the logistic regression framework to predict tissue temperature from measured acoustic emissions and tissue echogenicity.

2. ABLATION EXPERIMENTS AND DATA COLLECTION

2.1 Experimental Setup

The schematic of the experimental set up can be seen in Fig. 1. The primary component in this set up is a 32-element miniaturized image-ablate array (THX-3N) manufactured by Guided Therapy Systems in Mesa, AZ. This array can perform both thermal ablation and B-scan imaging with an active surface area of 2.3×49 mm^2 using the Iris imaging and ablation software provided by the same manufacturer. *Ex-vivo* bovine liver tissue was used for ablation. The tissue sample preparation was carried out according to a strict protocol. Bovine liver used was always less than 12 hours post mortem. For every ablation experiment a piece was freshly cut from the bovine liver tissue. Each piece was 7 (length)×3.5 (width)×3 (depth) cm^3. The tissue face directly exposed to the ultrasound beam hence had an area of 7×3.5 cm^2. It was ensured that the liver capsule was intact for this surface. The tissue sample was then placed in a latex condom (Probe Guard, Carter-Williams) which was partially filled with phosphate buffered saline (PBS). The saline used was degassed for a minimum of 90 minutes before use. After inserting the tissue inside the condom, it was carefully massaged to ensure minimum entrapment of bubbles inside the tissue. This tissue sample was then suspended in a tank of deionized water. The outer surface of the condom was then brushed to minimize the number of gas bubbles sticking to the same. The tissue sample and image-ablate array are suspended in the water tank such that the active surface of the array is parallel to and facing the liver capsule at a distance of 10-15 mm. A needle thermocouple (Ella CS type B) is inserted in the tissue sample parallel to the liver capsule 8-10 mm deep in the tissue from the liver capsule. Alignment and positioning of the thermocouple is done using real-time B-scan images captured by the image-ablate array operating in pulse-echo mode. The thermocouple is positioned such that the needle tip is at the center of the array aperture. This ensures that the thermocouple will measure the temperature in a region of the tissue incurring large heat deposition and hence a large increase in temperature during ablation procedure. Fig. 2 shows a B-scan image of the liver tissue with the thermocouple inserted. A C302 transducer manufactured by Panametrics is used as a passive cavitation detector (PCD). It is a 1 MHz, 25 mm diameter circular, unfocused transducer and is placed perpendicular to the direction in which the intense ultrasound beam is delivered by the image-ablate array. It is placed at a distance of about 10-15 mm from the tissue sample.

2.2 Data Collection Scheme

The Iris software enables control of tissue ablation. An experiment consists of exposing the tissue sample to several cycles of ablation and imaging actions. In each cycle the Iris system operates the miniaturized array in ablation (treatment or therapy) mode for 97-99% of time, after which it switches to the imaging mode. The Iris software was programmed to employ the center 16 elements of the 32-element, miniaturized array to produce a 3.1 MHz unfocused, continuous wave ultrasound beam in the ablation mode. When operating in the imaging mode, all 32 elements of the miniaturized array are used to form B-scan images using pulse-echo imaging. Acoustic emissions from the tissue are recorded using the 1 MHz PCD. The PCD is connected to a LeCroy WaveRunner digital oscilloscope which records signals at a sampling rate of 10 MHz. When the Iris software switches to imaging mode it generates a frame trigger causing the digital oscilloscope to record 1 million data samples from the PCD following a 100 ms delay. This delay ensures that acoustic emissions are recorded when the miniaturized array is delivering continuous wave ultrasound in a steady state. The same frame trigger also initializes a PC-based CompuScope CS 14200 A/D card (Gage Applied), which acquires RF echo traces at a sampling frequency of 33 MHz. This happens with the image-ablate array operating in the pulse-echo mode. These RF echo traces are used to reconstruct and post process B-scan images similar to Fig. 2.

Hence the acoustic emissions measured by PCD and the RF echo traces from the image-ablate array are captured synchronously. The tissue temperature is recorded asynchronously using an Omegaette HH206 digital data logger (by Omega Inc.). Temperature is sampled at approximately 1 Hz.

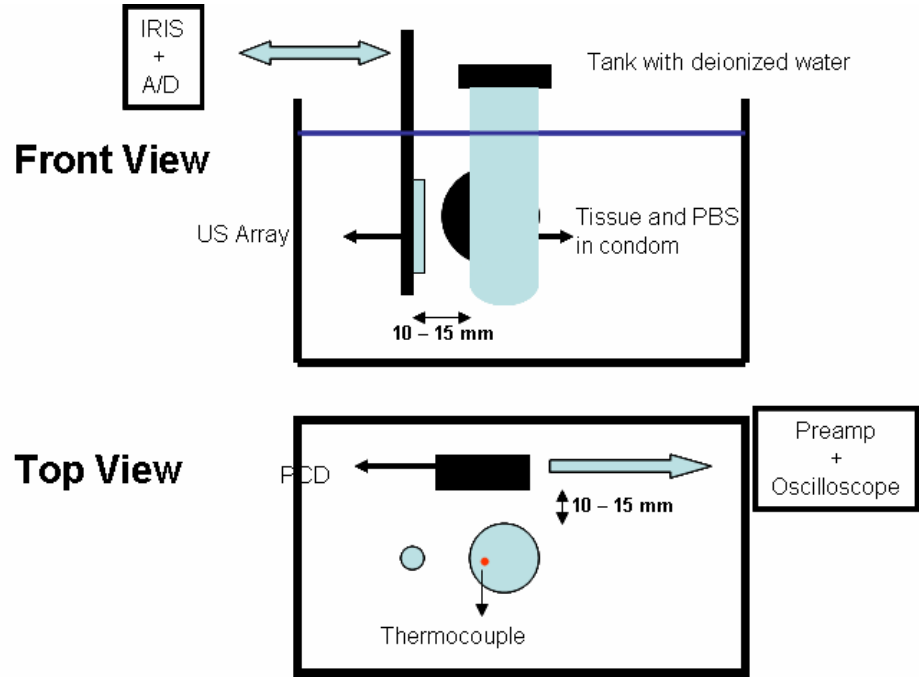

Figure 1: Schematic of experimental setup is presented in front and top views. Image-ablate array, PCD, tissue sample and thermocouple positions are indicated along with their DAQ hardware connections.

Results for a total number of 18 *ex-vivo* liver tissue experiments are reported in this paper. Six experiments each were conducted at three acoustic power levels of 16.2, 28.8 and 45.0 W. These power levels translate to 0.83, 1.10 and 1.38 MPa acoustic pressure amplitudes at a distance of 15 mm from the image-ablate array. Exposure time at 0.83 MPa was 20 minutes with the PCD data and RF echo traces recorded at a frame rate of 0.3 Hz. At 1.10 MPa the exposure time was 10 minutes and the frame rate was 0.6 Hz. Finally, at 1.1 MPa the exposure time was 10 minutes and the frame rate was 1.1 Hz. With increasing acoustic pressure (and power levels) the rate of heat deposition is increased. Hence exposure time is decreased and the frame rate is increased accordingly. Temperature, recorded asynchronously at 1 Hz, is interpolated to the frame rate for data analysis.

2.3 Data Analysis

Quantities measured during these experiments are acoustic emissions (recorded by PCD), B-scan images (reconstructed from RF echoes captured by CompuScope A/D card) and tissue temperature (measured by thermocouple). The acoustic emissions contain information which enables the monitoring of cavitation activity by generating a periodogram. At each frame trigger the WaveRunner Oscilloscope records 1 million data points from the PCD at 10 MHz and stores it in a binary file (.trc extension). During the course of each experiment 330 to 360 such files are saved. Data contained in each file is hence a snapshot of 100 ms of acoustic emissions at a given point of time during the experiment. A rectangular window 1000 points long, with zero overlap is applied to each file yielding 1000 "snippets" of the data. For each "snippet" a 1000–point Fast Fourier Transform (FFT) is computed. A periodogram is then ascertained by averaging the FFT squared values for these "snippets," and the spectrum energy is converted to dB, relative to the measured noise floor in each frequency band. This procedure when repeated for each binary file reveals energy content of various frequency components during at different time instants through an experiment. Change in energy content in three frequency ranges is calculated over time. Presence of stable cavitation presents as energy in the subharmonic frequency which is 1.55 MHz in these experiments.[10] Inertial cavitation gives rise to broadband activity.[10] The PCD response rolls

off after 1 MHz and hence the total energy contained between 0.3–1.1 MHz is calculated over entire experiment time. As tissue boiling is characterized by low frequency acoustic emissions, energy content between 20–40 kHz is calculated to monitor tissue boiling.[10] Fig. 3 shows changes in acoustic emissions in the above mentioned frequency ranges with respect to time.

At each frame trigger, RF echoes are captured and stored using the CompuScope A/D card. At each frame trigger, 32 2048-point RF echo traces (A-lines) are stored at 33 MHz which are converted into a B-scan image. First a Hilbert transform operation is performed and then the data is rearranged into 32×2048 pixels corresponding to an image width of about 25 mm and a depth of about 45 mm. One such image is generated per frame trigger. Changes in B-scan images during the experiment are of interest. For the region marked by the dotted box in Fig. 2 the grayscale values of the pixels are squared and then averaged. This average value is then converted to dB. This yields one mean grayscale value per frame trigger. This region of interest is about 25 (width)×22 (depth) mm^2 and is approximately centered on the thermocouple tip (see Fig. 2).

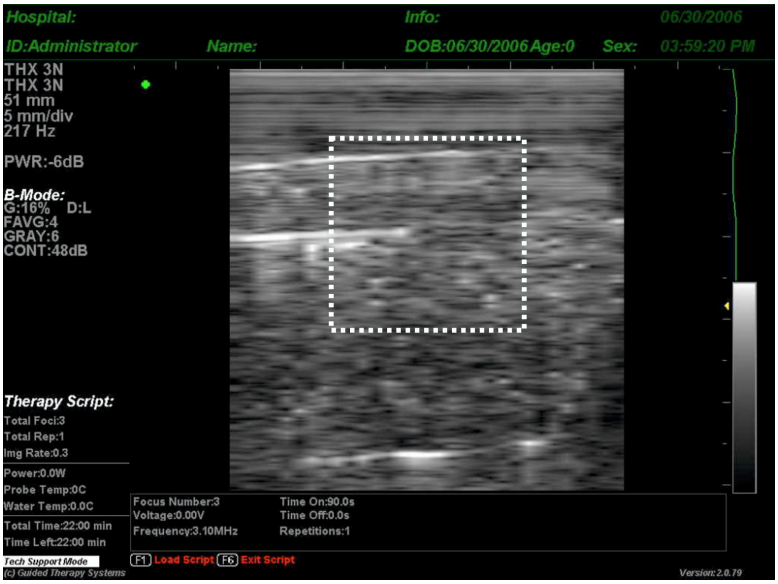

Figure 2: B-scan image of tissue captured buy image-ablate array. The dotted rectangular box is the region of interest for which change in mean grayscale value is computed over time. The bright line at the center of the dotted rectangle is the thermocouple. The bright line in the top portion of the dotted box is the tissue boundary.

3. DATA ANALYSIS

3.1 Correlation analysis for acoustic emissions and B-scan grayscale time-series

Linear correlation coefficients between temperature, broadband, subharmonic, low frequency and mean grayscale value are presented in Table 1. Correlation between temperature and subharmonic activity is statistically insignificant. All other correlations are statistically significant (p–value <0.01) though the correlation coefficients are not high.

Fig. 4 consists of scatter plots for temperature against broadband, subharmonic, low frequency and mean grayscale value. It is evident that there is no linear relation between temperature and these measured quantities. However, the data suggest a thresholding effect. A significant increase can be seen in the level of broadband and low frequency emissions and mean grayscale values when the temperature increases beyond 80^{o}C at the thermocouple. This is most pronounced in case of the highest acoustic pressure amplitude (1.4 MPa marked by red triangles). This makes sense intuitively, for the low frequency emissions are believed to be a consequence of tissue boiling.

The relationship between temperature and measured quantities also appears to be a function of the acoustic pressure amplitude. This is can be seen clearly in the scatter plot of subharmonic activity and temperature. For the lowest acoustic pressure amplitude (0.8 MPa) it can be seen that subharmonic activity is more pronounced for temperatures

between 45 and 60°C. However, for the highest acoustic pressure amplitude (1.4 MPa) high subharmonic activity occurs within a higher temperature range (75 to 110°C). As seen previously, the correlation between temperature and subharmonic activity is statistically insignificant. However, the thresholding nature of their relation seen in Fig. 4 can be exploited in a statistical model.

	Broadband	Subharmonic	Low Frequency	MGSV
Temperature	**0.419**	-0.00065	**0.527**	**0.455**

Table 1: Temporal correlation coefficient s between temperature, broadband activity, subharmonic activity, low frequency emissions and mean grayscale value. The statistically significant correlation coefficients are in bold. Their *p*-values are << 0.01 for a total of $N = 6179$ data points.

3.2 Logistic Regression Overview

Control of ablation treatment will be facilitated if tissue temperature can be predicted using noninvasively measurable quantities like acoustic emissions and B-scan grayscale values. An input/output model between these quantities is desired. The inputs to such a model could be broadband, subharmonic and low frequency activity, and mean grayscale values. These input variables (or covariates) are measured during the experiments. The acoustic pressure amplitude and treatment times are covariates which are known *a priori*. The model output (dependent variable or response) would be the predicted temperature. All the variables are continuous. The model most often used in such a scenario is multiple regression. Fig. 4 reveals the lack of a linear relation between temperature and measured variables. Hence a multiple regression model will not provide an acceptable representation of the input/output relation. One possible option is to use nonlinear curve-fitting to model the data. A less rigorous statistical model can be used to predict whether the tissue temperature has exceeded a certain stipulated value during the experiment. This can be achieved by use of logistic regression to model the data set.

Logistic regression can be used when the response variable is binary. Let $\mathbf{Y}$ be the binary response variable and $\mathbf{X}_1$, $\mathbf{X}_2$ and $\mathbf{X}_3$ be the covariates. They can be continuous or categorical (take values like 0, 1, 2 etc. or good, better, best, etc). Logistic regression will model the probability of $\mathbf{Y}$=1 or 0 as a function of the covariates:

$$\mathbf{P(Y = 1) = \exp(\beta_0 + \beta_1 * X_1 + \beta_2 * X_2 + \beta_3 * X_3)/(1 + \exp(\beta_0 + \beta_1 * X_1 + \beta_2 * X_2 + \beta_3 * X_3)).}$$

Here $\boldsymbol{\beta}$'s are called the model parameters. These parameters can be estimated for a given data set using the method of maximum likelihood.

3.3 Input/Output Models using Logistic Regression

For the experiments presented here, the output variable is temperature, which is continuous. In order to use logistic regression it is converted to binary. Since tissue ablation and necrosis set in when the tissue temperature exceeds approximately 60°C,[9] this can be used as a temperature threshold. If the temperature exceeds 60°C the response variable is considered equal to 1, else 0. As seen in Fig. 4, for temperatures above 80°C we see an increase in low frequency emissions. This would imply that there may be boiling in some regions of the tissue. Hence 80°C may also be a useful threshold. Logistic regression is used to here compute the probability that the temperature is above or below either of these thresholds for a given set of input variables.

Several input/output models using logistic regression are employed in this paper using different covariates. As mentioned earlier, some of the covariates are measured, while some are known *a priori*. It would be worthwhile to compare temperature prediction based on measured quantities and *a priori* variables. It will help appraise the usefulness of information yielded through the measured quantities. The models developed in this paper have the following covariates:

Model 1: Broadband, subharmonic, low frequency, mean grayscale value (measured quantities only)

Model 2: Acoustic pressure amplitude, time elapsed during experiment (quantities known *a priori*)

Model 3: Broadband, subharmonic, low frequency, mean grayscale value, acoustic pressure amplitude, time elapsed during experiment

Model 4: Broadband, subharmonic, low frequency, mean grayscale value, acoustic pressure amplitude (categorical variable)

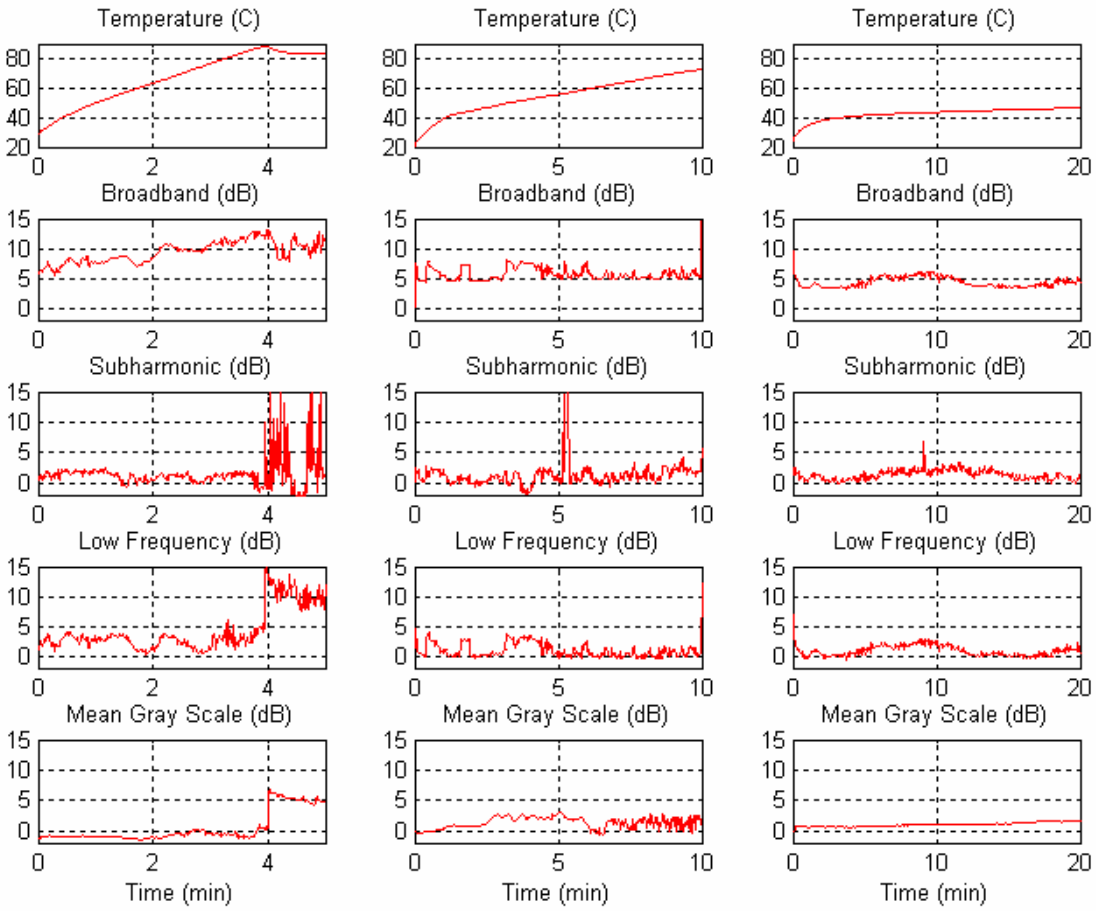

Figure 3: Tissue temperature, broadband, subharmonic, low frequency and MGSV values varying with time during an exposure. Representative graphs for each acoustic pressure level (1.4 MPa on left, 1.1 MPa on center and 0.8 MPa on right).

Four models each are fitted for temperature thresholds at 60°C and 80°C. The total number of experiments included in this paper are 18. This amounts to 6179 data points. 15 experiments, 5 at each of the three acoustic pressure amplitudes are used here to build the statistical models. The total number of data points used to build the models is 5149. Broadband, subharmonic and low frequency activity, and mean grayscale value are expressed in decibels (dB) relative to measured background levels. Estimated acoustic pressure amplitude is expressed in MPa and elapsed treatment time is expressed in minutes. When pressure is treated as a categorical variable with three distinct levels, the pressure covariate is replaced by three dummy variables. Let the dummy variables be $\mathbf{P_1}$, $\mathbf{P_2}$ and $\mathbf{P_3}$ and parameters associated with them be $\boldsymbol{\beta_{P1}}$, $\boldsymbol{\beta_{P2}}$ and $\boldsymbol{\beta_{P3}}$:

Pressure = $\mathbf{P_1}^* \boldsymbol{\beta_{P1}} + \mathbf{P_2}^* \boldsymbol{\beta_{P2}} + \mathbf{P_3}^* \boldsymbol{\beta_{P3}}$.

When pressure amplitude is 0.8 MPa, $\mathbf{P_1} = 1$ while $\mathbf{P_2}$, $\mathbf{P_3} = 0$. When pressure amplitude is 1.1 MPa, $\mathbf{P_2} = 1$and $\mathbf{P_1}$, $\mathbf{P_3} = 0$. Similarly $\mathbf{P_3} = 1$ when pressure amplitude is 1.4 MPa while $\mathbf{P_1}$, $\mathbf{P_2} = 0$. The logistic regression model presented here has $\boldsymbol{\beta_{P3}} = 0$.

All the logistic regression models presented here are estimated using SAS 9.1.3. When a covariate was found to be statistically insignificant, it was dropped and the model was rebuilt using the remaining covariates. Statistical models are then tested on the 5149 data points used to build them. They are also tested on the remaining 3 experiments (not used in model building), which is a total of 1030 data points. Tables 2 and 3 list the parameters for each of the above

four models. Tables 4 and 5 indicate model performance on the data included and excluded in parameter estimation, respectively.

The model performance is gauged as follows:

- If probability value generated by the model is greater than 0.5, tissue temperature is assumed to be greater than threshold value
- Correct Prediction: **P** > 0.5 and Temp > Threshold OR **P** < 0.5 and Temp < Threshold
- False Negative: **P** < 0.5 and Temp > Threshold
- False Positive: **P** > 0.5 and Temp < Threshold

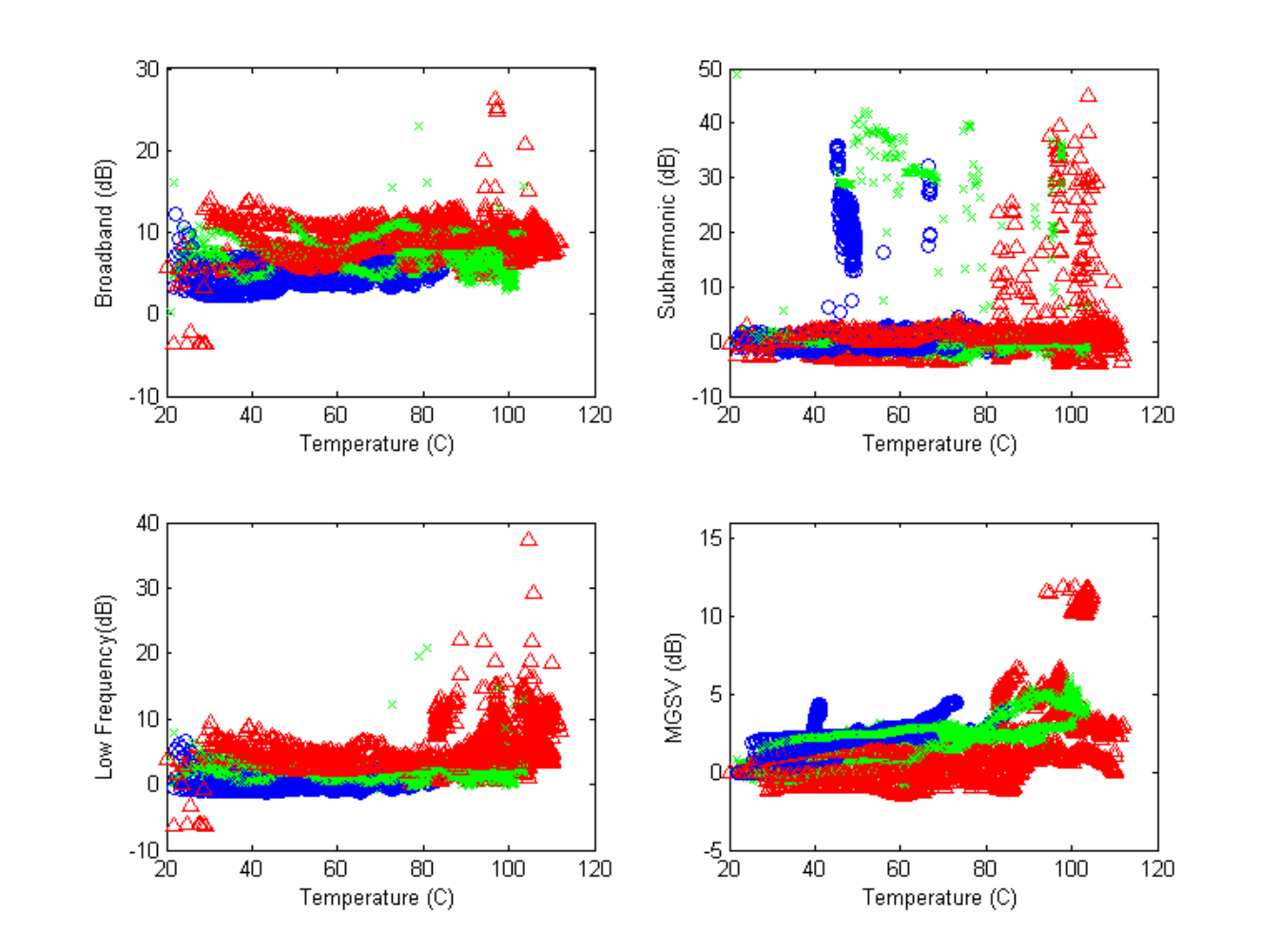

Figure 4: Scatter plots of temperature against broadband, subharmonic, low frequency and MGSV for 18 experiments. 1.4 MPa in red, 1.1 MPa in green and 0.8 MPa in blue.

4. DISCUSSION

Performance of a model is evaluated by the number of correct predictions it makes on the model building and testing data sets. Model 1 uses only the measured variables. For the data set used in model estimation, its prediction accuracy is 75% for the 60°C threshold and 83% for the 80°C threshold. The broadband activity, low frequency emissions and MGSV increase significantly when temperature at the thermocouple is above 80°C. However for a temperature range of 30-70°C, these quantities do not vary as significantly (see Fig. 4). There is some variation with respect to acoustic pressure (scatter plots of three different colors do not completely overlap in 30-70°C range in Fig. 4). However Model 1

does not contain pressure information. This could be the reason for its greater accuracy at the higher temperature threshold.

Model 2 uses only the variables known *a priori*. It performs slightly better at the lower temperature threshold (79%) than the higher threshold (77%). The thermocouple temperature changes monotonically. Higher temperatures are observed for higher acoustic pressures. Also higher temperatures are recorded when tissue is exposed for longer duration. Model 2 contains information for both the pressure and treatment time. This may be the reason for its comparable performance at both thresholds. Model 3 uses both the measured variables and the variables known *a priori*. For the data set used in model building, prediction accuracy of Model 3 is higher than Models 1 and 2 (82% at 60°C and 85% at 80°C), as its parameters were estimated using greater information than Models 1 and 2.

	Intercept	**Broadband**	**Subharm.**	**Low Freq.**	**MGSV**	**Pressure**	**Time**
Model 1	-3.319	0.2295	-0.0349	0.3109	0.8866	--	--
Model 2	-11.5001	--	--	--		8.9971	0.3633
Model 3	-13.4105	Insignificant	-0.029	Insignificant	0.9823	9.7106	0.2591
Model 4	-2.0049	Insignificant	-0.0292	0.1001	1.3253	-1.7882 0.0253	--

Table 2: Parameters of logistic regression models for the 60°C threshold (N = 5149), shown with one model per row and one covariate per column. Covariates not used in building a model are denoted by "--". "Insignificant" implies that the covariate was found to be statistically insignificant.

	Intercept	**Broadband**	**Subharm.**	**Low Freq.**	**MGSV**	**Pressure**	**Time**
Model 1	-4.3071	Insignificant	-0.012	0.7917	0.8192	--	--
Model 2	-19.7575	--	--	--	--	14.0237	0.4671
Model 3	-24.1502	-0.2161	0.024	0.3306	1.3416	16.6187	0.3727
Model 4	-3.5075	-0.215	Insignificant	0.4946	1.3663	-2.5621 0.2644	--

Table 3: Parameters of logistic regression models for the 80°C threshold (N = 5149), shown as in Table 2.

	Temp > 60			**Temp > 80**		
	Correct	False Positive	False Negative	Correct	False Positive	False Negative
Model 1	3844	671	634	4260	202	687
Model 2	4056	660	433	3967	627	555
Model 3	4203	589	357	4395	299	455
Model 4	4004	572	573	4372	234	543

Table 4: Performance of fitted models on data used during model parameter estimation (N = 5149).

	Temp > 60			**Temp > 80**		
	Correct	False Positive	False Negative	Correct	False Positive	False Negative
Model 1	697	88	245	978	11	41
Model 2	715	315	0	793	237	0
Model 3	784	162	84	989	2	39
Model 4	713	114	203	979	8	43

Table 5: Performance of fitted models on test data set of 1030 points.

Models using information from only the measured covariates may be better suited for ablation control. The covariates known *a priori* are assumed to take certain values over each experiment (for example acoustic pressure is assumed to be 0.8, 1.1 or 1.4 MPa). However, the *in situ* pressure amplitude will vary due to tissue structure and acoustic properties. Fig. 3 shows representative plots for acoustic emissions, tissue echogenicity and tissue temperature when *ex vivo* bovine liver is exposed to the three estimated acoustic pressure amplitudes from the image-ablate array. Behavior for each of these measured quantities was found to depend strongly on the acoustic amplitude.[10] Hence the estimated acoustic

pressure level could be used as a categorical covariate. Two parameters can be seen associated with the pressure covariate for Model 4 in Tables 2 and 3. On the data used in model construction, Model 4 performs better than Model 1 as only the former contains information about pressure level. The performance of Model 4 (78% at 60°C and 85% at 80°C) is comparable to Model 3, especially at the higher threshold.

On the test data set (1030 data points not used in model building), Model 1 fares better than Model 2 for the 60°C threshold and worse for the 80°C threshold. For the test data set, Model 2 predicts no false negatives. This implies that Model 2 never underestimates the temperature in the test data set. Model 3 performs better than both Models 1 and 2. Performance of Model 4 is comparable to Model 3 and better than Model 2 for the 80°C threshold.

A false negative implies that the probability value which the model outputs is less than 0.5, however the actual tissue temperature is below threshold level. This erroneous prediction may however prevent undertreatment, especially in case of the 60°C threshold. If false negatives are also considered to be an acceptable output, prediction success for Model 4 is 89% for the 60°C threshold and 99% for 80°C threshold in the test data set. Corresponding numbers for the model building data set are 89% and 95%. Models 1 and 3 show similar success rates, but Model 2, which employed only *a priori* information, is much less successful, with 30% false positive predictions for the test data set at the 60°C threshold and 23% false positive predictions for the 80°C threshold.

MGSV is a dominant covariate for both thresholds, especially at higher pressures. This agrees with the observation that tissue echogenicity increases significantly during high pressure exposures. The parameter associated with low frequency emissions is more dominant for the 80°C threshold than for the 60°C threshold in all cases. This is consistent with the observation that the low frequency emissions are indicative of tissue boiling. For the 60°C threshold, the broadband activity becomes statistically insignificant for Models 3 and 4. This can be attributed to the fact that significant change in broadband emissions is not seen at lower temperatures.

Model 4	**Intercept**	**Broadband**	**Subharm.**	**Low Freq.**	**MGSV**	**Pressure**
Mean	-2.0054	Insignificant	-0.0292	0.1001	1.3256	-1.7885 0.0254
Std Dev	0.029	--	0.002	0.008	0.013	0.016 0.011

Table 6: Mean and standard deviation of parameter values during cross validation (Temp > 60°C).

Model 4	**Intercept**	**Broadband**	**Subharm.**	**Low Freq.**	**MGSV**	**Pressure**
Mean	-3.5084	-0.2151	Insignificant	0.4947	1.3668	-2.5629 0.2644
Std Dev	0.063	0.007	--	0.013	0.014	0.039 0.018

Table 7: Mean and standard deviation of parameter values during cross validation (Temp > 80°C).

To further test the validity of this logistic regression approach, performance of Model 4 is investigated in greater detail. Goodness–of–fit for logistic regression is ascertained by the Hosmer and Lemeshow statistic which gives a *p*–value based on the Chi–Square distribution.[11] In case of a good fit this value has to be less than 0.05. In case of Model 4, the corresponding *p*–value was less than 0.0001 for both thresholds, consistent with the high percentage of correct prediction. Robustness of Model 4 is tested through cross-validation. The entire data set used for building the model (N=5149) is randomly divided into 10 equal parts. Nine parts are used to build a model. This procedure is performed 10 times, leaving out $1/10^{th}$ of the data during each iteration. The model parameters calculated during each iteration are then pooled together to evaluate their mean value and standard deviations. A robust model would imply that the standard deviations are small. In case of Model 4 for both thresholds the standard deviations are a minimum of one order of magnitude below that mean parameter values (see Tables 6 and 7).

Successful implementation of logistic regression involves converting the continuous response variables (tissue temperature) to a binary form, causing loss of information. Other input/output models with nonlinear curve fitting techniques could be employed without this information loss. Time series models which involve a "system identification" approach may also prove useful.

5. CONCLUSIONS

Tissue temperature may be predicted from measured acoustic emissions and ultrasound B-scans using a statistical input /output model. Temporal correlation between tissue temperature, acoustic emissions and tissue echogenicity, measured during unfocused ultrasound ablation experiments, is statistically significant but weak. Relations between temperature and the measured quantities are nonlinear. Hence a logistic regression model is appropriate to predict whether the tissue temperature exceeds a certain threshold during an experiment. The measured acoustic emissions and tissue echogenicity can be used as inputs to this model. Models based only on measured quantities, only on *a priori* known variables, and on both measured and *a priori* known variables have been presented for two temperature thresholds. Models which use all the variables exhibit the best prediction accuracy. However comparable prediction accuracy is observed if the *a priori* estimated acoustic pressure is used as a categorical variable along with the measured quantities. Models using only measured quantities also performed well, with a small number of false positive predictions for each temperature threshold.

REFERENCES

1. J. E. Kennedy, G. R. ter Haar *et al.,* "High intensity focused ultrasound: surgery of the future?" Br. Journal of Radiology, Volume 76, 590-599 (2003).
2. M. Kudo *et al.,* "Local ablation therapy for hepatocellular carcinoma: current status and future perspective," Journal of Gastroenterology, Volume 39, 205-214 (2004).
3. I. R. S. Makin, T. D. Mast *et al.,* "Miniaturized ultrasound arrays for interstitial ablation and imaging," Ultras. Med. Biol. Volume 31, 1539–1550 (2005).
4. D. Melodelima, J. Y. Chapelon *et al.,* "Combination of thermal and cavitation effects to generate deep lesions with an endocavitary applicator using a plane transducer: *ex vivo* studies," Ultras. Med. Biol. Volume 30, 103-111 (2004).
5. T. G. Leighton, *The Acoustic Bubble*, Academic Press, San Diego, CA, 1994.
6. A. Anand, L. Byrd *et al.,* "In situ thermal parameter estimation for HIFU therapy planning and treatment monitoring," IEEE Ultrasonics Symposium**,** Volume 1**,** 137- 140 (2004).
7. B. A. Rabkin *et al.,* "Hyperecho in ultrasound images of HIFU therapy: involvement of cavitation," Ultras. Med. Biol. Volume 31, 947 (2005).
8. C. R. Thomas, C. H. Farny *et al.,* "Dynamics and control of cavitation during high-intensity focused ultrasound application," Acoustics Research Letters Online [DOI: 10.1121/1.1901744] Published Online 24 June 2005.
9. T. D. Mast, I. R. S. Makin *et al.,* "Bulk ablation of soft tissue with intense ultrasound: modeling and experiments," J. Acoust. Soc. Am. Volume 118, 2715-2724 (2005).
10. T. D. Mast, V. A. Salgaonkar *et al.,* "Measurements of cavitation dose, echogenicity, and temperature during ultrasound ablation," in Proceedings of the 6th International Symposium on Therapeutic Ultrasound (2006).
11. D. W. Hosmer, S. Lemeshow, *Applied Regression Analysi*s, Wiley Series in Probability and Statistics, 2nd Edition, 2000.